NEA/NSC/DOC(95)03/IV
Volume IV

LEU-SOL-THERM-005

BORON CARBIDE ABSORBER RODS IN URANIUM (5.64% ^{235}U) NITRATE SOLUTION

Evaluators

Anatoli Tsiboulia
Yevgeniy Rozhikhin
Victor Gurin
Institute of Physics and Power Engineering

Internal Reviewer
Mark Nikolaev

Independent Reviewers

Virginia F. Dean
Consultant to INEEL

Calvin M. Hopper
Oak Ridge National Laboratory

BORON CARBIDE ABSORBER RODS IN URANIUM (5.64% ^{235}U) NITRATE SOLUTION

IDENTIFICATION NUMBER: LEU-SOL-THERM-005 SPECTRA

KEY WORDS: absorber, absorber rods, acceptable, boron, boron carbide, critical experiment, cylinder, homogeneous, low-enriched, moderated, nitric acid, solution, thermal, uranium, uranyl nitrate, water-reflected

1.0 DETAILED DESCRIPTION

1.1 Overview of Experiment

A large number of critical experiments with absorber elements of different types in uranium nitrate solution of different enrichments and concentrations were performed in 1961 - 1963 at the Solution Physical Facility of the Institute of Physics and Power Engineering (IPPE), Obninsk, Russia. The purpose of these experiments was to determine the effects of enrichment, concentration, geometry, neutron reflection, and type, diameter, number, and arrangement of absorber rods on the critical mass of light-water-moderated homogeneous uranyl nitrate solutions. The experiments included ones with a central boron carbide or cadmium rod, clusters of boron carbide rods, and triangular lattices of boron carbide rods in cylindrical tanks of different dimensions filled with solutions of uranyl nitrate.[a]

The three experiments included in this evaluation were performed with uranium enriched to 5.64 wt.% ^{235}U. Uranium nitrate solution with uranium concentration of 400.2 g/l was pumped into the core or inner tank, a stainless steel cylindrical tank with inner diameter 110 cm. One experiment was performed without absorber rods, another one with a central rod, and another one with a cluster of seven absorber rods arranged at the corners and center of a hexagon with a pitch of 31.8 cm, inserted in the center of the core tank. There was a thick side and bottom water reflector in these experiments. All three configurations are considered to be acceptable for use as criticality safety benchmark experiments.

Experiments performed using the same tank and absorber rods with uranium enrichments of 10% and 89% are reported in evaluations LEU-SOL-THERM-006 and HEU-SOL-THERM-035.

1.2 Description of Experimental Configuration

A diagram of the critical assembly is shown in Figure 1 (vertical cut). The experiment was performed in the same room as the other uranium-solution experiments at IPPE (see Appendix B of

[a] See LEU-SOL-THERM-006, HEU-SOL-THERM-027, HEU-SOL-THERM-028, HEU-SOL-THERM-029, HEU-SOL-THERM-030, HEU-SOL-THERM-031, HEU-SOL-THERM-035, and HEU-SOL-THERM-037.

HEU-SOL-THERM-014). The room had dimensions $7.5 \times 5.5 \times 8.8$ m. The core central axis was 2 m from the north wall, 5.5 m from the south wall, and 2.75 m from the west and east walls. All the walls, the ceiling, and the floor were concrete. The thickness of the walls was approximately 100 cm, the thickness of the ceiling was 75 cm, and the thickness of the floor was 20 cm.

The critical assembly consisted of two open-topped coaxial cylindrical tanks. The core tank was 110.0 cm in inner diameter, 250.0 cm tall, with wall thickness 0.6 cm, and bottom thickness 1.5 cm. The reflector tank had 198.4 cm inner diameter, was 300 cm tall, with wall thickness 0.8 cm, and bottom thickness 1.0 cm. The core tank stood on a pedestal inside the reflector tank. The height of the pedestal was 36.0 cm. No other characteristics of the pedestal are not known. The reflector tank stood on the floor.

The core tank was partially filled with the aqueous solution of uranyl nitrate $UO_2(NO_3)_2$ with some excess of nitric acid (HNO_3). The reflector tank was filled with distilled water in all cases. The height of the water reflector measured from the bottom (inner surface) of the core tank was 108.0 cm.

The average inside diameter of the core tank was measured by filling the tank with a known volume of water and then measuring the water level. Several volumes were used to establish the inside diameter of the tank. The uncertainty of the core tank average inside diameter is $\pm$ 0.2 cm.

The core tank was filled with solution through a polyethylene feed pipe, with inner diameter 1.2 cm. The pipe wall thickness was 0.2 cm. The end of this pipe was positioned under the solution surface. Pumping the solution out of the tank was performed through a stainless steel pipe, with outer diameter 1.2 cm and wall thickness 0.15 cm. The pipes entered the tank from the top. These pipes are not shown in Figure 1.

The three experiments performed were: one without absorber rods; another one with central absorber rod; and another one with seven absorber rods at the corners and center of a hexagon with pitch 31.8 cm.

The absorber rods were stainless steel tubes with outer diameter of 5.5 cm, 255 cm long, with wall thickness 0.5 cm, and bottom thickness 0.7 cm. The reported uncertainty of the tube outer diameter is $\pm$ 1%. These tubes were filled with a powder of boron carbide.

The space between the absorber rods was ensured by two stainless steel lattice plates. These plates were 1.7 cm thick. The upper plate was placed on top of the core tank, as shown in Figure 1. The diameter of the upper plate was 115 cm. The lower plate lay on the bottom of the core tank. The diameter of this plate was 109.6 cm. There were 85 holes 5.55 cm in diameter arranged in a triangular lattice with pitch 10.6 cm for the absorber rods in these plates, as shown in Figure 2.

Three boron carbide control rods were suspended above the surface of the solution. The control rods were stainless steel tubes with outer diameter 3 cm and wall and bottom thickness 0.2 cm filled with boron carbide powder. The distance between the critical solution surface and the bottom of the control rods varied from 10 to 20 cm above the solution. Empty holes in the upper lattice plate were used for the boron carbide control rods. Where these rods were located exactly is not known.

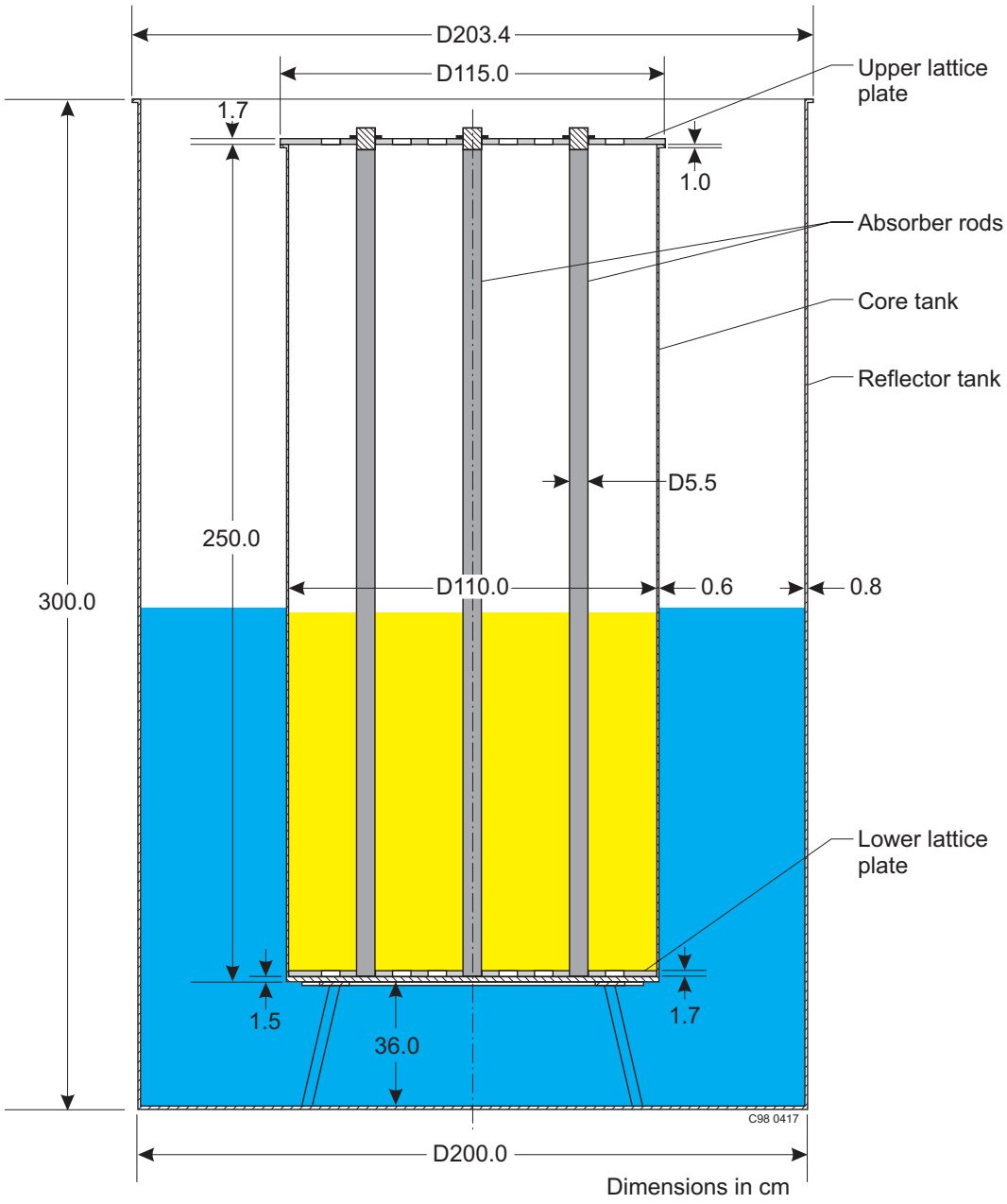

Figure 1. Critical Assembly (Case 3 - vertical cut).

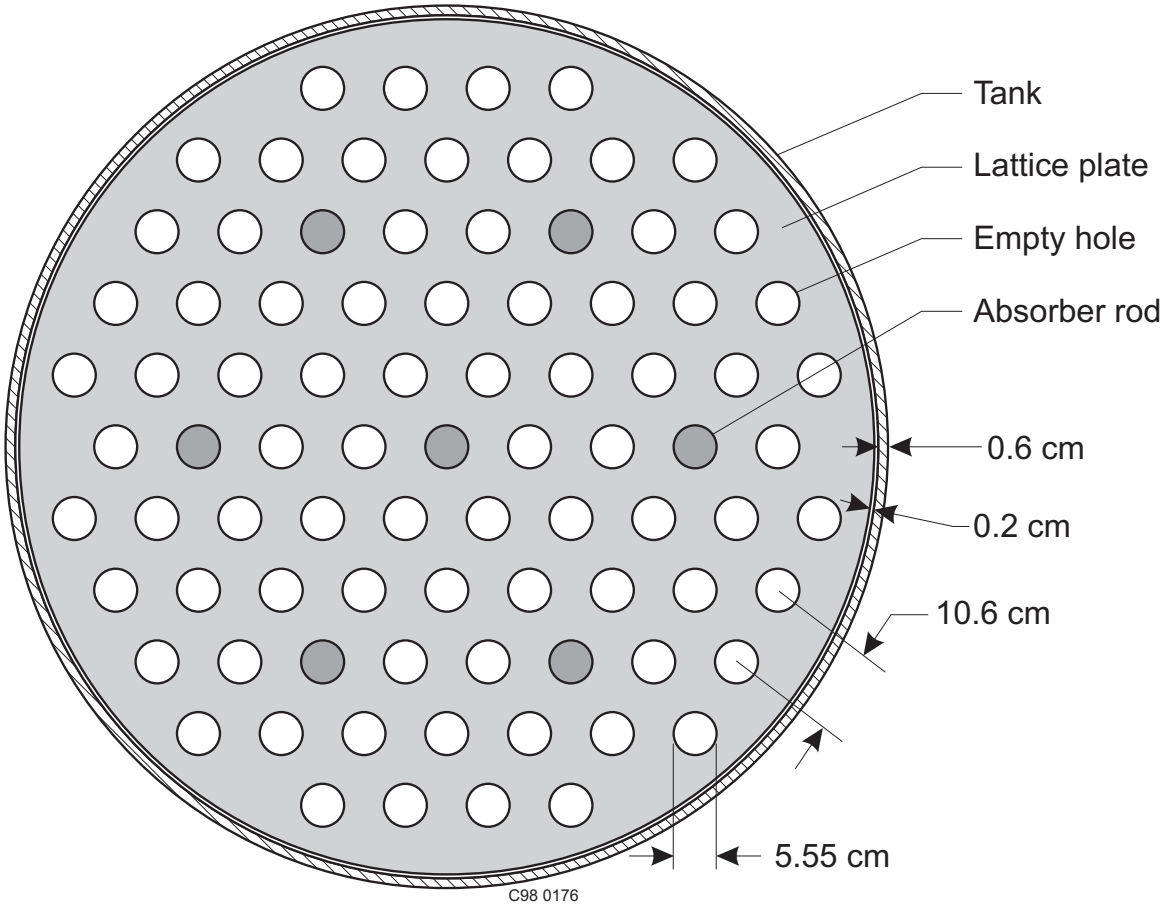

Figure 2. Core Tank of the Critical Assembly.
(Case 3 - horizontal cut through the lower lattice plate.)

Six ionization chambers of the control system were located in six "dry" vertical stainless steel tubes, 6.3 cm in diameter with wall thickness 1.5 mm, symmetrically arranged outside the core tank at a surface-to-surface distance of 20 cm from it. The elements of the control system are not shown in Figure 1.

There was no other apparatus or equipment in the room at the time of the experiment that might affect criticality.

More detailed description of the experimental room and safety/control-rod support system is given in Appendix B in HEU-SOL-THERM-014.

The typical procedure for determining the critical condition was as follows: The core tank, with absorber rods in place, was filled with uranyl nitrate solution portion by portion. The volume of a successive portion was determined from the reciprocal multiplication curve. Portions were small (the smallest sized portion was 0.05 liter) near criticality. The experiments were reported as

"critical" but further information about determining the critical condition was not retained. Other solution experiments performed at the facility were taken to a slightly supercritical state.

The experimental results obtained for the different experimental conditions are presented in Table 1.

Table 1. Critical Dimensions (see Figure 1).

Case Number	Number of Absorber Rods	Solution Volume, liters
1	none	548.0 ± 0.9
2	1	606.0 ± 1.0
3	7	983.0 ± 1.5

The experiments were performed at room temperature (approximately 20°C).

1.3 Description of Material Data

Low-enriched uranium was used in the experiments. The uranium isotopic composition is given in Table 2.

Table 2. Uranium Isotopic Composition.

Isotope	Wt.%
^{234}U	0.03 ± 0.02
^{235}U	5.64 ± 0.06
^{236}U	0.05 ± 0.03
^{238}U	94.28 ± 0.06
Total:	100.00

The uranium solution was uranyl nitrate, $UO_2(NO_3)_2$, from UO_2 dissolved in nitric acid (HNO_3) and diluted with distilled water. The solution density was measured by a float-type hydrometer with the value of one scale division equal to 0.001 g/cm^3. This value was adopted as the measure of the inaccuracy of the density determination.

The uranium concentration in the solution was measured by weighing U_3O_8 which was prepared by precipitation of ammonium diuranate and its heating. Two or three analyses were done. As usual, two or three small portions of the solution were taken from the core tank (usually from the bottom, middle, and top of the core) after criticality was achieved and then a complete analysis of the solution properties was performed in the chemical laboratory, located in the same building in a

neighboring room. The temperature in the chemical laboratory was the same as in the experimental room, therefore the density and uranium concentration of the solution remained constant. The range of the results was, as a rule, smaller than method inaccuracies. So the latter (± 0.5%) was adopted as a measure of the uncertainty of the uranium concentration determination. Determinations of chemical-methodology inaccuracies were done previously for a wide range of measured concentrations. (See, for example, HEU-SOL-THERM-014, HEU-SOL-THERM-015, HEU-SOL-THERM-016, HEU-SOL-THERM-017, HEU-SOL-THERM-018, and HEU-SOL-THERM-019.)

The concentration of free nitric acid in the solution was determined by the alkalimetric titration method. The uncertainty of this method is ± 1%.

Solution properties are given in Table 3.

Table 3. Solution Properties.

Uranium Concentration, grams/liter	Solution Density, grams/cm^3	Concentration of HNO_3, moles/liter
400.2 ± 2.0	1.590 ± 0.001	1.60 ± 0.02

All impurities in the solution were caused by the impurity of the uranyl nitrate used, not by water impurities. Concentrations of impurities in uranium dioxide determined by chemical analysis are given in Table 4. Because the uranium concentration was measured by a chemical method that can detect only uranium,[a] the measured uranium concentration did not include impurities.

[a] Personal communication, A. A. Krinitsin, analytical chemist IPPE, May, 1997.

Table 4. Concentrations of Impurities in Uranium Dioxide.

Element	Wt.%
Fe	0.0300
C	0.0150
Si	0.0050
Ni	0.0030
Ca	0.0015
Cu	0.0010
Mg	0.0010
N	0.0010
Al	0.0010
Mn	0.0003
Cr	0.0003
Co	0.0002
B	0.00001
Total:	0.05931

Natural boron was used in the experiments. The density of the boron carbide powder was 1.25 ± 0.13 g/cm^3.

The cylindrical tanks, absorber rod tubes, and auxiliary parts of the critical assemblies used in these experiments were made of 1X18H10T stainless steel. The composition and density of the stainless steel was determined by normative data on the steel 1X18H10T and was not analyzed specifically. Its composition and density, according to the USSR State Standard 5632-72, is given in Table 5. Cited inaccuracies are caused by possible deviations of the real composition from the normative one.

Table 5. Stainless Steel[(a)] Composition.

Element	Wt.%
Fe	69.1 ± 0.7
Cr	18.0 ± 0.5
Ni	10.0 ± 0.5
Mn	1.5 ± 0.2
Si	0.8 ± 0.1
Ti	0.6 ± 0.1
Total:	100.0

(a) Density is 7.93 ± 0.02 g/cm^3

1.4 Supplemental Experimental Measurements

No additional experimental data were found.

2.0 EVALUATION OF EXPERIMENTAL DATA

2.1 General Notes

The results of the considered experiments were collected from unclassified internal reports that are published in Reference 1. Additional experimental data were extracted from the internal IPPE reports and retained working books. Many questions were resolved in talks with experimenters and with analytical chemists.

2.2 Influence of Uncertainties in Experimental Parameters on Criticality

The uncertainty of k_{eff} due to reported measurement uncertainties for this set of experiments was calculated. These calculations were performed using one-dimensional cylindrical models of assemblies with critical buckling by means of the CRAB-1 code and three-dimensional HEX-Z models by means of the TRIGEX code with the ABBN-90[a] group cross sections set. Some results were additionally checked by the KENO-5A code.

Inaccuracy of the determination of criticality caused by uncertainties of the following parameters was estimated:

- isotopic composition of uranium;
- uranium concentration in solution;
- solution density;
- HNO_3 concentration in solution;
- impurity concentrations in solution;
- absorber material;
- absorber rods pitch;
- critical dimensions.

To determine the reactivity effect due to the uncertainty of the isotopic concentrations, data of Table 2 were used. The ^{235}U concentration was varied by ± 0.06 wt.% with a corresponding change of ^{238}U atomic density. The corresponding changes in k_{eff} are shown in Table 6 as Δk_{ε}.

To determine the reactivity effect due to the uncertainty of the uranium concentration in solution, data of Table 3 were used. The uranium concentration was varied by the uncertainty value of 2 g/liter. The corresponding changes in k_{eff} are shown in Table 6 as Δk_U.

To determine the reactivity effect due to the uncertainty of the solution density, data of Table 3 were used. The solution density was varied by ± 0.001 g/cm^3. The corresponding changes in k_{eff} are shown in Table 6 as Δk_{sol}.

[a] RSICC DLC-182 "ABBN-90: Multigroup Constant Set for Calculation of Neutron and Photon Radiation Fields and Functionals, Including the CONSYST2 Program."

To determine the reactivity effect due to the uncertainty of the HNO_3 concentration in solution, data of Table 3 were used. The concentration of HNO_3 was varied by the uncertainty value 0.02 moles/liter. The observed change in k_{eff} did not exceed 0.0006. The corresponding changes in k_{eff} are shown in Table 6 as Δk_{acid}.

As estimated by direct calculations, concentrations of impurities in the solution were so small that their influence on k_{eff} of the considered assemblies is ~ 0.01%. Thus it was not necessary to include the influence of uncertainties of these concentrations in the k_{eff} uncertainty. (The calculations with impurities included the additional nitrate ions bound to the impurities.)

To estimate the reactivity effect due to the uncertainty of the absorber material dimensions, it was supposed that the uncertainty of the outer diameter of the stainless steel tube is ± 1% (with constant wall thickness). The volume of the solution was conserved. This leads to change in the surface area of the absorber material. The calculated uncertainty was divided by the square root of the number of rods. The corresponding changes in k_{eff} are shown in Table 6 as Δk_s.

To estimate the reactivity effect due to the uncertainty of the wall thickness of the stainless steel tube of the absorber rod, it was supposed that the uncertainty of the wall thickness is ± 0.05 cm (± 10%). The calculated uncertainty was divided by the square root of the number of rods. The corresponding changes in k_{eff} are shown in Table 6 as Δk_w.

To estimate the reactivity effect due to the uncertainty of the pitch of the absorber rods for Case 3, the rod-separation value was changed by 0.1 cm. The calculated uncertainty was divided by the square root of the number of rods ($\sqrt{7}$). The corresponding changes in k_{eff} are shown in Table 6 as Δk_p.

To determine the reactivity effect due to the uncertainty of the solution volume, the solution heights were changed by the value that corresponds to the uncertainty of the solution volume given in Table 1 at the constant tank inner radius. The corresponding changes in k_{eff} are shown in Table 6 as Δk_h.

To determine the reactivity effect due to the uncertainty of the core tank inner radius, the value of inner radius was changed by 0.1 cm and the solution heights correspondingly were changed (thus the critical volumes were conserved). The tank thickness remained constant. The corresponding changes in k_{eff} are shown in Table 6 as Δk_r.

To estimate the reactivity effect due to the uncertainty of the core tank wall and bottom thickness, it was supposed that the uncertainty of the wall and bottom thickness of the tank is ± 10%. The corresponding changes in k_{eff} are shown in Table 6 as Δk_t.

The influence of the uncertainty in density of the absorber material was calculated by variation of the boron carbide density by ± 0.13 g/cm^3. The effect is shown in Table 6 as Δk_d.

The effect of the uncertainty in the isotopic composition of natural boron (19.1% to 20.3% ^{10}B) was also calculated. The effect is shown in Table 6 as Δk_b.

Because the solution density was measured at the time of the experiments, and because the effect of water-reflector density variation due to a large (10°C) temperature change was calculated to be negligible, there is no additional k_{eff} uncertainty due to uncertain temperature.

All Δk's were determined consistent with formulas provided in Section 3.0.

In Table 6 the constituents of the inaccuracy of k_{eff} are listed for all assemblies of the considered series. In the last column, the summary inaccuracy of k_{eff} is given

$$\Delta k = \sqrt{\Delta k_{\varepsilon}^2 + \Delta k_U^2 + \Delta k_{sol}^2 + \Delta k_{acid}^2 + \Delta k_s^2 + \Delta k_w^2 + \Delta k_p^2 + \Delta k_h^2 + \Delta k_r^2 + \Delta k_t^2 + \Delta k_d^2 + \Delta k_b^2}$$

Table 6. Constituents of the Inaccuracy of k_{eff} (percents).

Case	Δk_{ε}	Δk_U	Δk_{sol}	Δk_{acid}	Δk_s	Δk_w	Δk_p	Δk_h	Δk_r	Δk_t	Δk_d	Δk_b	Δk
1	0.39	0.12	0.01	0.05	--	--	--	0.02	0.03	0.04	--	--	0.41
2	0.46	0.16	0.01	0.05	0.04	0.01	--	0.02	0.04	0.04	0.03	0.05	0.50
3	0.51	0.29	0.01	0.06	0.13	0.12	0.05	0.03	0.04	0.05	0.05	0.05	0.63

Because sufficient data are known and uncertainties have been quantified as relatively small, the three configurations are acceptable benchmark experiments.

3.0 BENCHMARK SPECIFICATIONS

3.1 Description of Model

3.1.1 Description of Simplifications - The benchmark models were based on a series of simplifications to the actual experimental configurations. The following experimental details were omitted, after evaluating their influence on criticality during the benchmark specifications:

- impurities in fissile solution;
- small constructive details in and around the assembly, including the upper lattice plate, and reflection of neutrons from the room walls.

3.1.2 Influence of the Elimination of Impurities - As was pointed out in Section 2, the influence of solution impurities on k_{eff} was negligibly small. Thus impurities are not included in the benchmark models and no correction of k_{eff} was made.

3.1.3 Influence of the Elimination of the Experimental Surroundings - Because the thick water reflector was used, the experimental surroundings (i.e., room wall, ionization-chamber tubes) had no noticeable influence on the k_{eff} of the considered assemblies. The effect of removing the control rods located above the solution surface was estimated using the KENO-5A code. The effect was found to be less than 0.1% with approximately the same uncertainty. Because the exact positions of the control rods in the experiments are not known, the additional 0.1% uncertainty is included in the benchmark-model k_{eff}'s. The influence of removing the fill and drain tubes was estimated earlier (see HEU-SOL-THERM-014, HEU-SOL-THERM-015, HEU-SOL-THERM-016, HEU-SOL-THERM-017, HEU-SOL-THERM-018, and HEU-SOL-THERM-019) using perturbation theory. It was assumed that in the considered series the fill and drain tubes also do not influence criticality. Making the top surfaces of the two tanks and absorber rods coplanar, thereby reducing the height of the rods by 5 cm and reducing the height of the reflector tank by 13 cm, to simplify the model was judged to have negligible effect.

3.2 Dimensions

The benchmark models of the experiments are shown in Figures 3 through 8. The model is two open-top coaxial stainless steel cylindrical tanks. The core tank has inner diameter 110.0 cm, wall thickness 0.6 cm, bottom thickness 1.5 cm, is 250.0 cm tall, filled with solution of uranyl nitrate to the height (measured from the inner surface of the tank bottom) shown in Table 7. The reflector tank, with inner diameter 198.4 cm, wall thickness 0.8 cm, bottom thickness 1.0 cm, 287.0 cm tall, is filled with water to the height (measured from the inner surface of the core tank bottom) 108.0 cm. The distance between the inner surface of the reflector tank bottom and the outer surface of the core tank bottom is 36.0 cm.

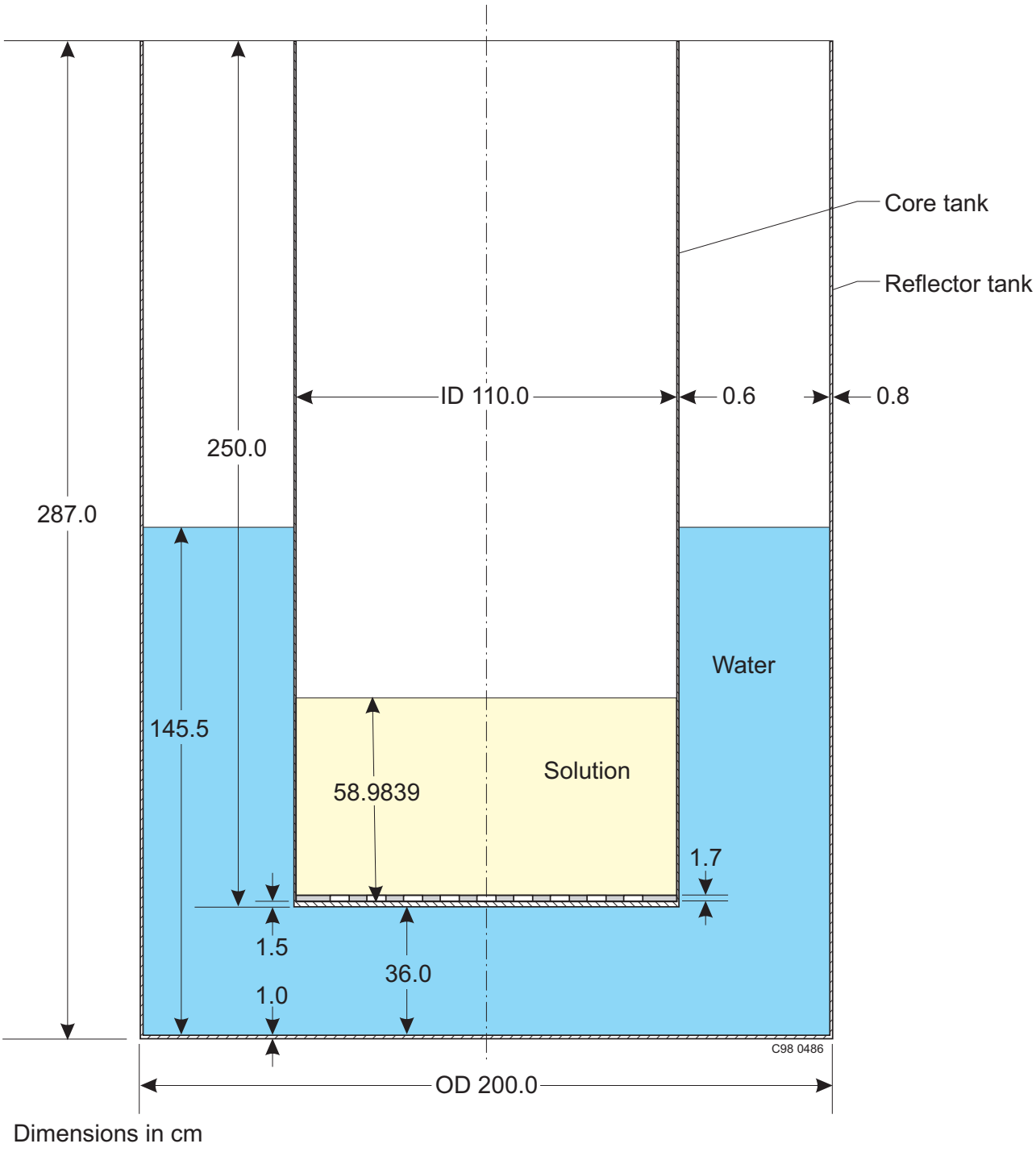

Figure 3. Benchmark Model of Case 1 (vertical cut).

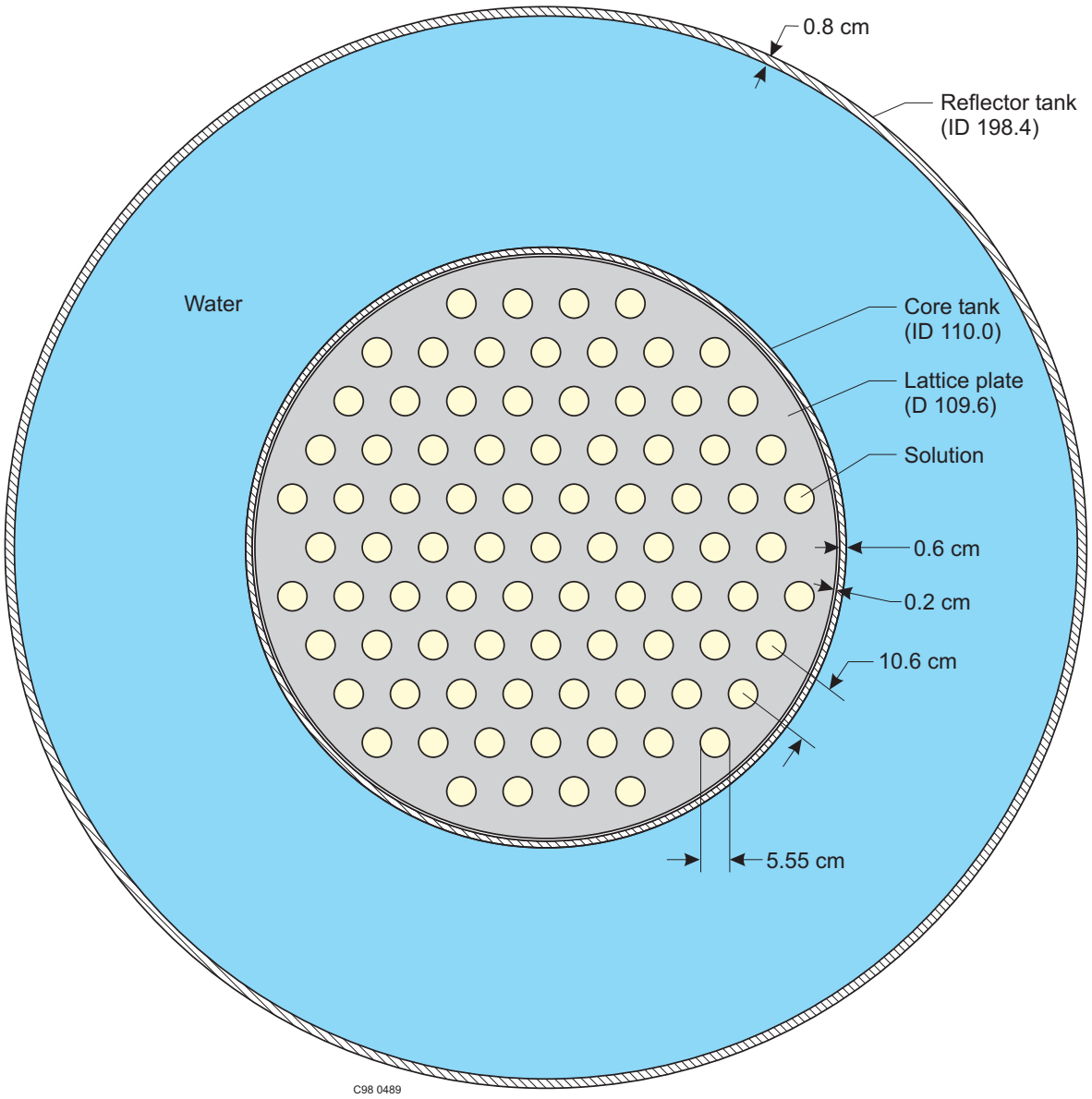

Figure 4. Benchmark Model of Case 1 (horizontal cut through lattice plate).

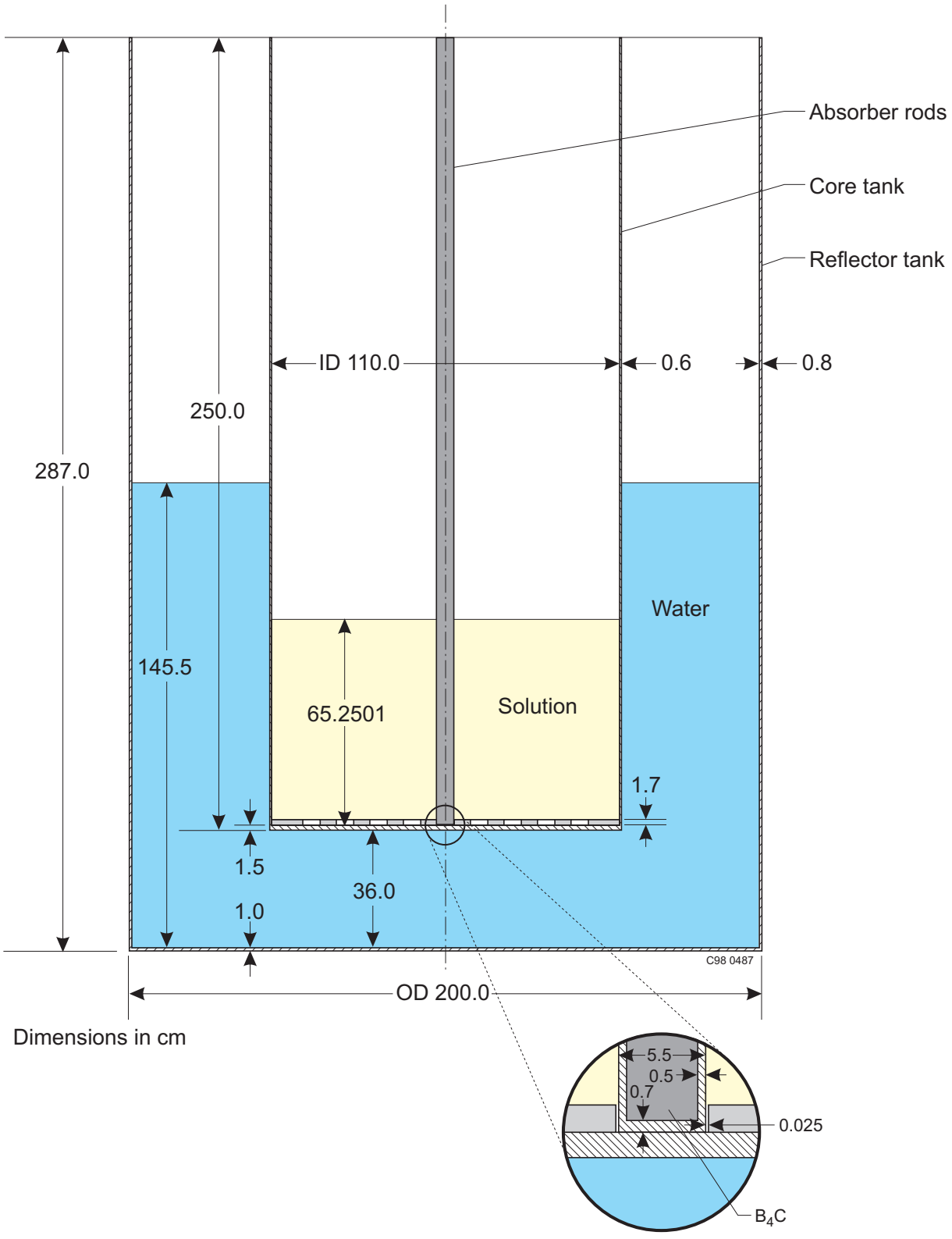

Figure 5. Benchmark Model of Case 2 (vertical cut).

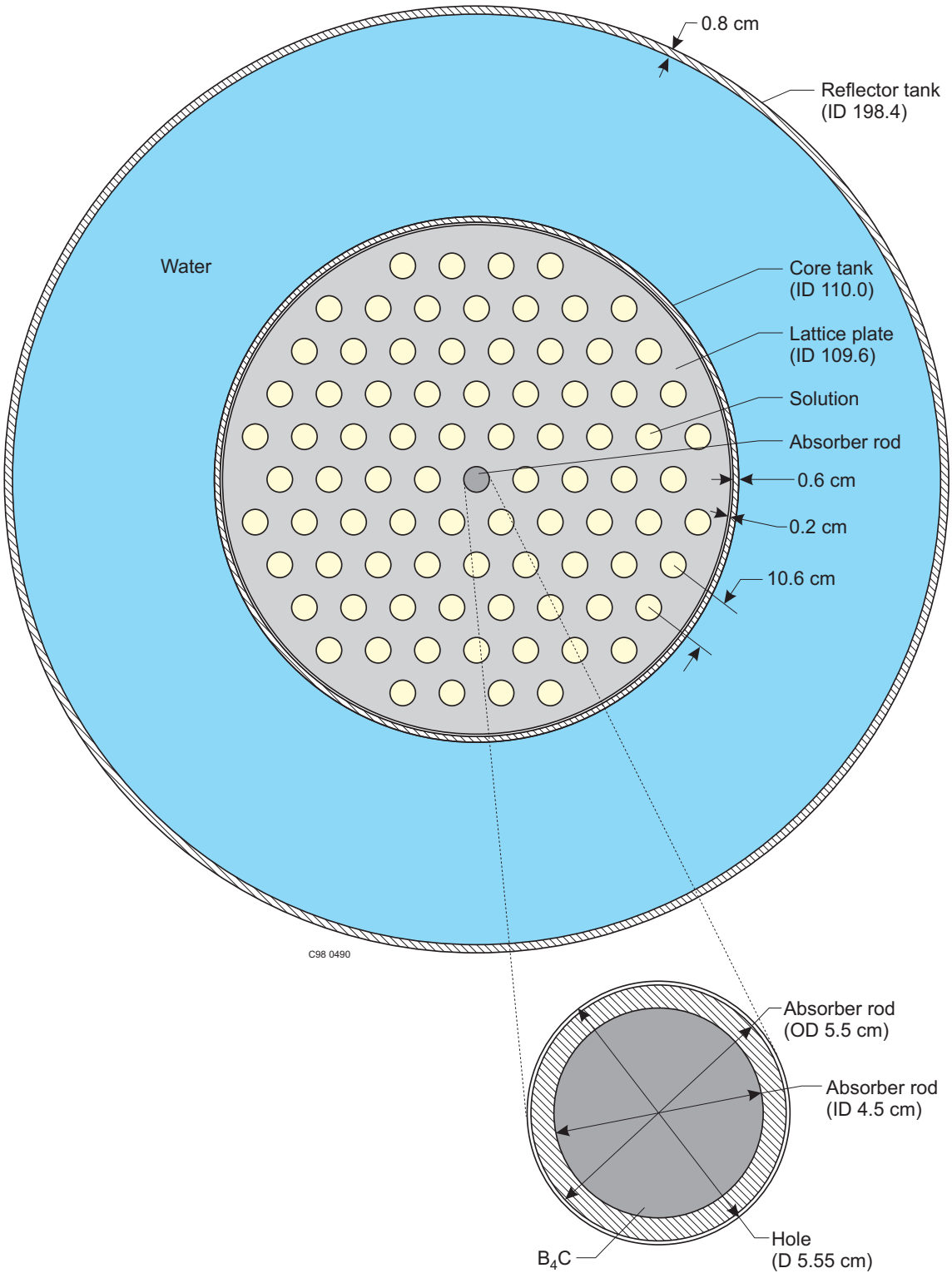

Figure 6. Benchmark Model of Case 2 (horizontal cut through lattice plate).

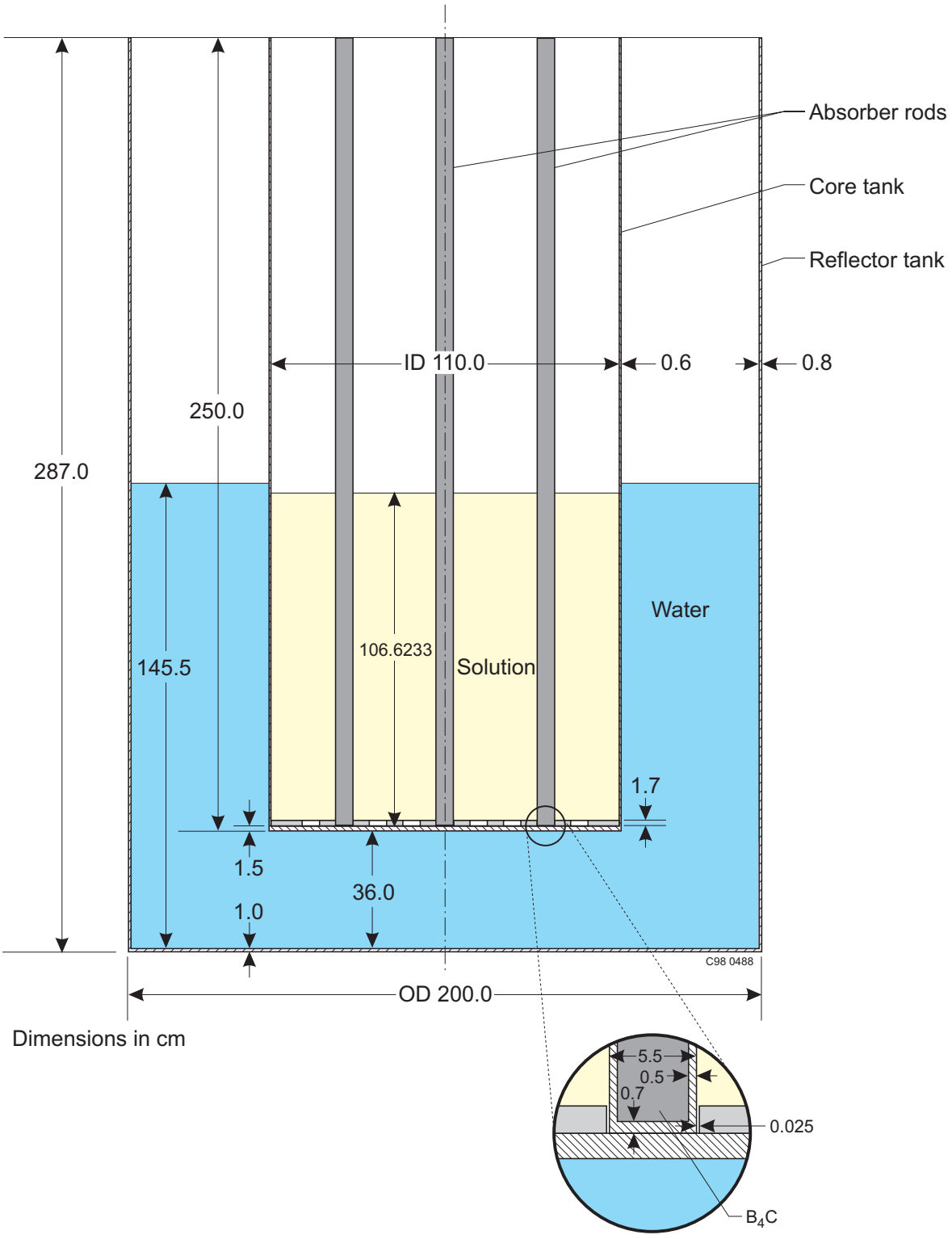

Figure 7. Benchmark Model of Case 3 (vertical cut).

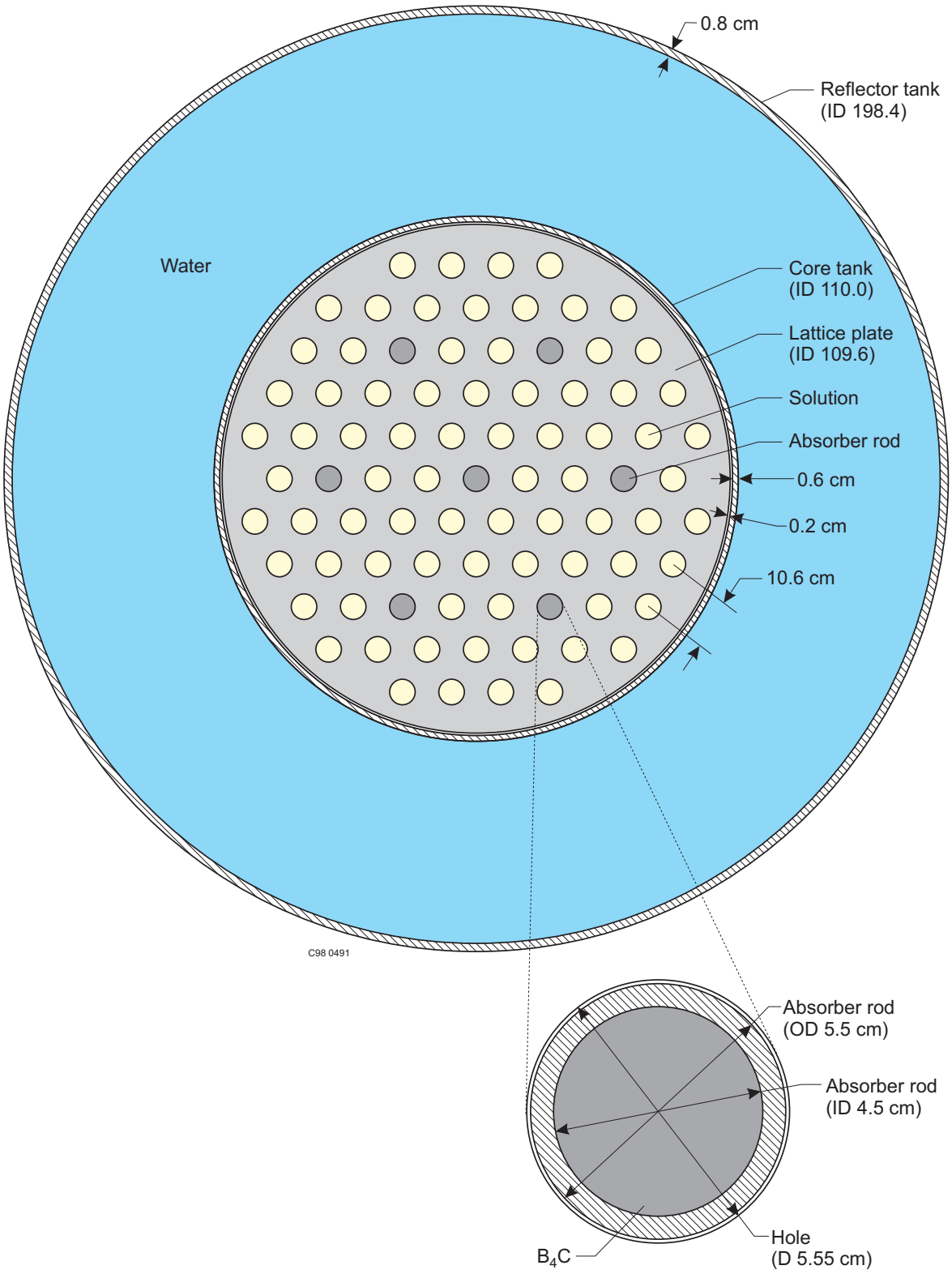

Figure 8. Benchmark Model of Case 3 (horizontal cut).

Table 7. Geometrical Sizes of Benchmark Models.

Case Number	Number of Absorber Rods	Solution Height, cm
1	0	58.9839
2	1	65.2501
3	7	106.6233

There are three experimental configurations. The first one is without absorber rods. One absorber rod is inserted in the center of the core tank in the second configuration. A cluster of seven boron absorber rods in a hexagonal lattice (one rod at each corner of the hexagon and one rod at the center) is inserted in the center of the core tank in the third configuration. The pitch of the lattice is 31.8 cm.

The boron absorber rods are stainless steel tubes with outer diameter of 5.5 cm, wall thickness 0.5 cm, and bottom thickness 0.7 cm, 248.5 cm long, filled with natural boron carbide. The absorber rods extend to the bottom of the core tank. The top surface of the absorber rods is coplanar with the top surfaces of the core and reflector tanks.

The lower stainless steel lattice plate is also included in the three benchmark models. This plate is lying on the bottom of the core tank. It has diameter 109.6 cm and is 1.7 cm thick. There are 85 holes in the plate arranged in a hexagonal lattice with pitch 10.6 cm. The arrangement of the holes in the plate is shown in Figures 4, 6, and 8. The holes have diameter 5.55 cm.

3.3 Material Data

3.3.1 Core Nuclear Densities - The nuclear densities of the individual uranium isotopes are given by

$$N_i = \frac{W_{f,i}\ \rho_U\ N_A}{A_{w,i}}, \text{ for i} = {}^{234}\text{U}, {}^{235}\text{U}, {}^{236}\text{U}, {}^{238}\text{U}$$

where N_i is the nuclear density of isotope "i";
ρ_U is the uranium mass density in solution in g/cm^3 (see Table 3);
$W_{f,i}$ is the weight fraction of isotope "i" (see wt.%'s in Table 2);
$A_{w,i}$ is the atomic mass of isotope "i";
N_A is Avogadro's number.

The mass density of uranyl nitrate ($UO_2(NO_3)_2$) is given by

$$\rho_{UO2(NO3)2} = \frac{\rho_U \; M_{w,UO2(NO3)2}}{A_{w,U}}$$

where $A_{w,U}$ is the average atomic weight of the uranium, and
$M_{w,UO2(NO3)2}$ is the molecular weight of uranyl nitrate.

The mass density of nitric acid, HNO_3, in grams per cubic centimeter is given by

$$\rho_{HNO3} = 0.001 \cdot M_{w,HNO3} \cdot M_{HNO3}$$

where $M_{w,HNO3}$ is the molecular weight of nitric acid, and
M_{HNO3} is the concentration of HNO_3 in moles/liter (see Table 3).

The mass density of water in solution can be then determined by difference

$$\rho_{H2O} = \rho_{solution} - \rho_{UO2(NO3)2} - \rho_{HNO3}$$

The total atom densities of nitrogen (N_N), oxygen (N_O), and hydrogen (N_H) are then determined by the following formulas:

$$N_N = 2 \left(N_{U234} + N_{U235} + N_{U236} + N_{U238} \right) + 0.001 \cdot M_{HNO3} \cdot N_A$$

$$N_O = 2 \left(N_{U235} + N_{U234} + N_{U236} + N_{U238} \right) + \frac{\rho_{H2O} \; N_A}{M_{w,H2O}} + 3 N_N$$

$$N_H = N_A \left(2 \frac{\rho_{H2O}}{M_{w,H2O}} + \frac{\rho_{HNO3}}{M_{w,HNO3}} \right)$$

Here $M_{w,H2O}$ is the molecular weight of water, and ρ_{H2O}, ρ_{HNO3} in grams per cubic centimeter are calculated by the above formulas.

Using the above equations solution atom densities were calculated. Results of these calculations are given in Table 8.

Table 8. Calculated Atom Densities for 400.2 gU/l Solution.

Element	Atom Density, atoms/(barn × cm)
^{234}U	3.0893×10^{-7}
^{235}U	5.7830×10^{-5}
^{236}U	5.1050×10^{-7}
^{238}U	9.5450×10^{-4}
N	2.9898×10^{-3}
O	3.8624×10^{-2}
H	5.6221×10^{-2}

3.3.2 Boron Carbide Atom Densities - Atom densities of boron carbide B_4C were calculated using the following isotopic composition[a] of natural boron: ^{10}B - 19.9 at.%; ^{11}B - 80.1 at.%, and density of 1.25 g/cm^3. Boron carbide atom densities are given in Table 9.

Table 9. Atom Densities of Boron Carbide.

Element	Atom Density, atoms/(barn × cm)
^{10}B	1.0844×10^{-2}
^{11}B	4.3648×10^{-2}
C	1.3623×10^{-2}

3.3.3 Water Reflector Atom Density - The density of the water was selected for the temperature and pressure at which the experiment was conducted. The temperature of the water was 20°C (293 K), and pressure was approximately 0.1 MPa at the time of the experiment. Therefore the estimated water density was 0.9983 g/cm^3. Water atom densities are given in Table 10.

Table 10. Atom Densities of Water Reflector.

Element	Atom Density, atoms/(barn × cm)
H	6.6742×10^{-2}
O	3.3371×10^{-2}

[a] "Chart of the Nuclides," Fourteen Edition, General Electric Company, 1989.

3.3.4 Atom Densities of the Structure - Atom densities of stainless steel constituents were calculated from weight percents given in Table 5 and density of 7.93 g/cm^3. Data are given in Table 11.

Table 11. Atom Densities for Stainless Steel.

Element	Atom Density, atoms/(barn × cm)
Fe	5.9088×10^{-2}
Cr	1.6532×10^{-2}
Ni	8.1369×10^{-3}
Mn	1.3039×10^{-3}
Si	1.3603×10^{-3}
Ti	5.9844×10^{-4}

3.4 Temperature Data

All experiments were performed at room temperature (approximately 20°C). The temperature of 300 K was assumed for calculations.

3.5 Experimental and Benchmark-Model k_{eff}

Experimental critical parameters correspond to criticality: $k_{eff} = 1$. Uncertainties of experimental data result in an uncertainty of k_{eff}, as described in Section 2. Benchmark-model simplifications led to the additional 0.1% uncertainty of k_{eff}. Benchmark-model k_{eff}'s are shown in Table 12.

Table 12. Benchmark-Model k_{eff} Values.

Case Number	Benchmark-Model k_{eff}
1	1.0000 ± 0.0042
2	1.0000 ± 0.0051
3	1.0000 ± 0.0064

4.0 RESULTS OF SAMPLE CALCULATIONS

The results of calculations of k_{eff} of the benchmark models are given in Tables 13.a and 13.b. Details of the calculations including code input listings are provided in Appendix A.

Table 13.a. Sample Calculation Results (Russian Federation).[(a)]

Code (Cross Section Set) → Configuration ↓	KENO (ABBN-93)
1	0.9978 ± 0.0005
2	0.9990 ± 0.0005
3	0.9992 ± 0.0005

(a) Results supplied by Yevgeniy Rozhikhin, IPPE.

Table 13.b. Sample Calculation Result (United States).[(a)]

Code (Cross Section Set) → Configuration ↓	KENO (27-Group ENDF/B-IV)	MCNP (Continuous Energy ENDF/B-V)
1	0.9961 ± 0.0005	0.9983 ± 0.0005
2	0.9964 ± 0.0005	0.9986 ± 0.0005
3	0.9946 ± 0.0005	0.9999 ± 0.0005

(a) Results supplied by Yevgeniy Rozhikhin, IPPE.

5.0 REFERENCES

1. Дубовский Б. Г., Камаев А. В., Кузнецов Ф. М. и др. Критические параметры систем с делящимися веществами и ядерная безопасность. Справочник. Москва, Атомиздат, 1966. (Dubovskii B. G., Kamaev A. V., Kuznetsov F. M. et al., "Critical Parameters of Systems with Fissile Materials and Nuclear Safety. Handbook." Moscow. Atomizdat, 1966, in Russian.)

APPENDIX A: TYPICAL INPUT LISTINGS

A.1 KENO Input Listings

299-Group ABBN-93 Cross Sections

KENO-5A with the ABBN-93 299-group cross sections was run using 1020 generations of neutrons with 1000 neutrons each. Twenty generations were skipped before averaging, so the result is the average of 1,000,000 neutron histories.

27-Group ENDF/B-IV Cross Sections

The 27-group inputs given below are for the KENO-5A code as run with the ORNL SCALE4.3 code system using the CSAS option. The problems were run with 1,000,000 active and 20,000 inactive histories (1000 active generations, twenty skipped generations, and 1000 histories per generation).

KENO-5A Input Listing for Case 1 of Table 13.b (27-Energy-Group ENDF/B-IV Cross Sections).

```
=csas25
leu-sol-therm-005-01
27groupndf4 infhommedium
u-234 1 0 3.0893E-07 end
u-235 1 0 5.7830E-05 end
u-236 1 0 5.1050E-07 end
u-238 1 0 9.5450E-04 end
n     1 0 2.9898E-03 end
o     1 0 3.8624E-02 end
h     1 0 5.6221E-02 end
fe    2 0 5.9088E-02 end
cr    2 0 1.6532E-02 end
ni    2 0 8.1369E-03 end
mn    2 0 1.3039E-03 end
si    2 0 1.3603E-03 end
ti    2 0 5.9844E-04 end
h     3 0 6.6742E-02 end
o     3 0 3.3371E-02 end
b-10  4 0 1.0844E-02 end
b-11  4 0 4.3648E-02 end
c     4 0 1.3623E-02 end
end comp
leu-sol-therm-005-01
read param
tme=360
gen=1020
npg=1000
nsk=20
fdn=yes
far=yes
plt=no
end param
read geometry
unit   11
cylinder 1 1   2.775                      1.7     0.
cuboid   2 1   5.3    -5.3     3.     -3.      1.7     0.
'       .      .      .      .      .      .      .
unit   61
array  61      0.     0.     0.
unit   71
array  71      0.     0.     0.
unit   81
array  81      0.     0.     0.
unit   91
array  91      0.     0.     0.
unit  101
array 101      0.     0.     0.
'       .      .      .      .      .      .      .
unit  999
cylinder 0 1  55.                       248.5   108.
cylinder 2 1  55.6                      248.5   108.
'       .      .      .      .      .      .      .
global unit 1000
cylinder 2 1  54.8                        1.7     0.
hole  61     -21.2   -49.89934640058   0.
hole  71     -37.1   -39.71947712046   0.
hole  81     -42.4   -30.53960784035   0.
hole  91     -47.7   -21.35973856023   0.
hole 101      -53.   -12.17986928012   0.
hole  91     -47.7   -3.               0.
hole 101     -53.0    6.179869280115   0.
hole  91     -47.7    15.35973856023   0.
hole  81     -42.4    24.53960784035   0.
hole  71     -37.1    33.71947712046   0.
```

KENO-5A Input Listing for Case 1 of Table 13.b (27-Energy-Group ENDF/B-IV Cross Sections) (cont'd).

```
hole  61     -21.2    42.89934640058   0.
cylinder 1 1  55.                      58.9839  0.
cylinder 0 1  55.                     108.      0.
cylinder 2 1  55.6                    108.     -1.5
cylinder 3 1  99.2                    108.    -37.5
cylinder 0 1  99.2                    248.5   -37.5
hole 999       0.     0.      0.
cylinder 2 1 100.                     248.5   -38.5
end geometry
read array
ara= 61  nux= 4 nuy= 1 nuz=1  fill f11 end fill
ara= 71  nux= 7 nuy= 1 nuz=1  fill f11 end fill
ara= 81  nux= 8 nuy= 1 nuz=1  fill f11 end fill
ara= 91  nux= 9 nuy= 1 nuz=1  fill f11 end fill
ara=101  nux=10 nuy= 1 nuz=1  fill f11 end fill
end array
read plot
scr=yes
ttl='x-z slice at y=0.0 with x across and z down'
xul=-101.0  yul=   0.0   zul= 250.0
xlr= 101.0  ylr=   0.0   zlr= -40.0
uax=1.0 wdn=-1.0
nax=800 lpi=10 end
ttl='x-y slice at z=10.0 with x across and y down'
xul=-101.0  yul= 101.0   zul=  10.0
xlr= 101.0  ylr=-101.0   zlr=  10.0
uax=1.0 vdn=-1.0
nax=800 lpi=10 end
ttl='x-y slice at z=1.0 with x across and y down'
xul= -60.0  yul=  60.0   zul=   1.0
xlr=  60.0  ylr= -60.0   zlr=   1.0
uax=1.0 vdn=-1.0
nax=800 lpi=10 end
end plot
end data
end
```

KENO-5A Input Listing for Case 2 of Table 13.b (27-Energy-Group ENDF/B-IV Cross Sections).

```
=csas25
leu-sol-therm-005-02
27groupndf4 infhommedium
u-234 1 0 3.0893E-07 end
u-235 1 0 5.7830E-05 end
u-236 1 0 5.1050E-07 end
u-238 1 0 9.5450E-04 end
n     1 0 2.9898E-03 end
o     1 0 3.8624E-02 end
h     1 0 5.6221E-02 end
fe    2 0 5.9088E-02 end
cr    2 0 1.6532E-02 end
ni    2 0 8.1369E-03 end
mn    2 0 1.3039E-03 end
si    2 0 1.3603E-03 end
ti    2 0 5.9844E-04 end
h     3 0 6.6742E-02 end
o     3 0 3.3371E-02 end
b-10  4 0 1.0844E-02 end
b-11  4 0 4.3648E-02 end
c     4 0 1.3623E-02 end
end comp
leu-sol-therm-005-02
read param
tme=360
gen=1020
npg=1000
nsk=20
fdn=yes
far=yes
plt=no
end param
read geometry
unit   11
cylinder 1 1   2.775                    1.7     0.
cuboid   2 1   5.3    -5.3     3.     -3.      1.7     0.
unit   21
cylinder 4 1   2.25                     1.7     0.7
cylinder 2 1   2.75                     1.7     0.
cylinder 1 1   2.775                    1.7     0.
cuboid   2 1   5.3    -5.3     3.     -3.      1.7     0.
unit   22
cylinder 4 1   2.25                     65.2501  1.7
cylinder 2 1   2.75                     65.2501  1.7
unit   23
cylinder 4 1   2.25                     108.     65.2501
cylinder 2 1   2.75                     108.     65.2501
unit   24
cylinder 4 1   2.25                     248.5   108.
cylinder 2 1   2.75                     248.5   108.
'      .      .      .      .      .      .      .
unit   61
array  61      0.     0.     0.
unit   71
array  71      0.     0.     0.
unit   81
array  81      0.     0.     0.
unit   91
array  91      0.     0.     0.
unit  101
array 101      0.     0.     0.
unit  111
array 111      0.     0.     0.
'      .      .      .      .      .      .      .      .
```

KENO-5A Input Listing for Case 2 of Table 13.b (27-Energy-Group ENDF/B-IV Cross Sections) (cont'd).

```
unit  999
cylinder 0 1  55.                       248.5   108.
hole  24       0.      0.             0.
cylinder 2 1  55.6                      248.5   108.
'       .       .       .       .       .       .       .
global unit 1000
cylinder 2 1  54.8                       1.7     0.
hole  61     -21.2   -49.89934640058   0.
hole  71     -37.1   -39.71947712046   0.
hole  81     -42.4   -30.53960784035   0.
hole  91     -47.7   -21.35973856023   0.
hole 101     -53.    -12.17986928012   0.
hole 111     -47.7   -3.               0.
hole 101     -53.0    6.179869280115   0.
hole  91     -47.7    15.35973856023   0.
hole  81     -42.4    24.53960784035   0.
hole  71     -37.1    33.71947712046   0.
hole  61     -21.2    42.89934640058   0.
cylinder 1 1  55.                       65.2501  0.
hole  22       0.      0.             0.
cylinder 0 1  55.                       108.      0.
hole  23       0.      0.             0.
cylinder 2 1  55.6                      108.     -1.5
cylinder 3 1  99.2                      108.    -37.5
cylinder 0 1  99.2                      248.5   -37.5
hole 999       0.      0.      0.
cylinder 2 1 100.                       248.5   -38.5
end geometry
read array
ara= 61  nux= 4 nuy= 1 nuz=1  fill f11 end fill
ara= 71  nux= 7 nuy= 1 nuz=1  fill f11 end fill
ara= 81  nux= 8 nuy= 1 nuz=1  fill f11 end fill
ara= 91  nux= 9 nuy= 1 nuz=1  fill f11 end fill
ara=101  nux=10 nuy= 1 nuz=1  fill f11 end fill
ara=111  nux= 9 nuy= 1 nuz=1  fill 4r11 21 4r11 end fill
end array
read plot
scr=yes
ttl='x-z slice at y=0.0 with x across and z down'
xul=-101.0  yul=   0.0   zul= 250.0
xlr= 101.0  ylr=   0.0   zlr= -40.0
uax=1.0 wdn=-1.0
nax=800 lpi=10 end
ttl='x-y slice at z=10.0 with x across and y down'
xul=-101.0  yul= 101.0   zul=  10.0
xlr= 101.0  ylr=-101.0   zlr=  10.0
uax=1.0 vdn=-1.0
nax=800 lpi=10 end
ttl='x-y slice at z=1.0 with x across and y down'
xul= -60.0  yul=  60.0   zul=   1.0
xlr=  60.0  ylr= -60.0   zlr=   1.0
uax=1.0 vdn=-1.0
nax=800 lpi=10 end
end plot
end data
end
```

KENO-5A Input Listing for Case 3 of Table 13.b (27-Energy-Group ENDF/B-IV Cross Sections).

```
=csas25
leu-sol-therm-005-03
27groupndf4 infhommedium
u-234 1 0 3.0893E-07 end
u-235 1 0 5.7830E-05 end
u-236 1 0 5.1050E-07 end
u-238 1 0 9.5450E-04 end
n     1 0 2.9898E-03 end
o     1 0 3.8624E-02 end
h     1 0 5.6221E-02 end
fe    2 0 5.9088E-02 end
cr    2 0 1.6532E-02 end
ni    2 0 8.1369E-03 end
mn    2 0 1.3039E-03 end
si    2 0 1.3603E-03 end
ti    2 0 5.9844E-04 end
h     3 0 6.6742E-02 end
o     3 0 3.3371E-02 end
b-10  4 0 1.0844E-02 end
b-11  4 0 4.3648E-02 end
c     4 0 1.3623E-02 end
end comp
leu-sol-therm-005-03
read param
tme=360
gen=1020
npg=1000
nsk=20
fdn=yes
far=yes
plt=no
end param
read geometry
unit   11
cylinder 1 1   2.775                    1.7     0.
cuboid   2 1   5.3    -5.3     3.     -3.      1.7     0.
unit   21
cylinder 4 1   2.25                     1.7     0.7
cylinder 2 1   2.75                     1.7     0.
cylinder 1 1   2.775                    1.7     0.
cuboid   2 1   5.3    -5.3     3.     -3.      1.7     0.
unit   22
cylinder 4 1   2.25                     106.6233  1.7
cylinder 2 1   2.75                     106.6233  1.7
unit   23
cylinder 4 1   2.25                     108.    106.6233
cylinder 2 1   2.75                     108.    106.6233
unit   24
cylinder 4 1   2.25                     248.5   108.
cylinder 2 1   2.75                     248.5   108.
'      .     .     .     .     .     .     .
unit   61
array  61      0.     0.     0.
unit   71
array  71      0.     0.     0.
unit   81
array  81      0.     0.     0.
unit   91
array  91      0.     0.     0.
unit  101
array 101      0.     0.     0.
unit  111
array 111      0.     0.     0.
'      .     .     .     .     .     .     .     .
```

KENO-5A Input Listing for Case 3 of Table 13.b (27-Energy-Group ENDF/B-IV Cross Sections) (cont'd).

```
unit  999
cylinder 0 1  55.                        248.5   108.
hole  24       0.      0.             0.
hole  24     -31.8     0.             0.
hole  24     -15.9    27.53960784035   0.
hole  24      15.9    27.53960784035   0.
hole  24      31.8     0.             0.
hole  24      15.9   -27.53960784035   0.
hole  24     -15.9   -27.53960784035   0.
cylinder 2 1  55.6                     248.5   108.
'       .      .      .      .      .      .      .      .
global unit 1000
cylinder 2 1  54.8                       1.7     0.
hole  61     -21.2   -49.89934640058   0.
hole  71     -37.1   -39.71947712046   0.
hole  81     -42.4   -30.53960784035   0.
hole  91     -47.7   -21.35973856023   0.
hole 101      -53.   -12.17986928012   0.
hole 111     -47.7   -3.              0.
hole 101     -53.0    6.179869280115   0.
hole  91     -47.7    15.35973856023   0.
hole  81     -42.4    24.53960784035   0.
hole  71     -37.1    33.71947712046   0.
hole  61     -21.2    42.89934640058   0.
cylinder 1 1  55.                        106.6233  0.
hole  22       0.      0.             0.
hole  22     -31.8     0.             0.
hole  22     -15.9    27.53960784035   0.
hole  22      15.9    27.53960784035   0.
hole  22      31.8     0.             0.
hole  22      15.9   -27.53960784035   0.
hole  22     -15.9   -27.53960784035   0.
cylinder 0 1  55.                        108.      0.
hole  23       0.      0.             0.
hole  23     -31.8     0.             0.
hole  23     -15.9    27.53960784035   0.
hole  23      15.9    27.53960784035   0.
hole  23      31.8     0.             0.
hole  23      15.9   -27.53960784035   0.
hole  23     -15.9   -27.53960784035   0.
cylinder 2 1  55.6                       108.     -1.5
cylinder 3 1  99.2                       108.    -37.5
cylinder 0 1  99.2                       248.5   -37.5
hole 999       0.      0.      0.
cylinder 2 1 100.                        248.5   -38.5
end geometry
read array
ara= 61  nux= 4 nuy= 1 nuz=1  fill f11 end fill
ara= 71  nux= 7 nuy= 1 nuz=1  fill f11 end fill
ara= 81  nux= 8 nuy= 1 nuz=1  fill 2r11 21 11 n4 end fill
ara= 91  nux= 9 nuy= 1 nuz=1  fill f11 end fill
ara=101  nux=10 nuy= 1 nuz=1  fill f11 end fill
ara=111  nux= 9 nuy= 1 nuz=1  fill 11 21 11 2q3 end fill
end array
read plot
scr=yes
ttl='x-z slice at y=0.0 with x across and z down'
xul=-101.0  yul=   0.0   zul= 250.0
xlr= 101.0  ylr=   0.0   zlr= -40.0
uax=1.0 wdn=-1.0
nax=800 lpi=10 end
ttl='x-y slice at z=10.0 with x across and y down'
xul=-101.0  yul= 101.0   zul=  10.0
xlr= 101.0  ylr=-101.0   zlr=  10.0
```

KENO-5A Input Listing for Case 3 of Table 13.b (27-Energy-Group ENDF/B-IV Cross Sections) (cont'd).

```
uax=1.0 vdn=-1.0
nax=800 lpi=10 end
ttl='x-y slice at z=1.0 with x across and y down'
xul= -60.0  yul=  60.0   zul=   1.0
xlr=  60.0  ylr= -60.0   zlr=   1.0
uax=1.0 vdn=-1.0
nax=800 lpi=10 end
end plot
end data
end
```

A.2 MCNP Input Listings

The MCNP4A calculation with continuous-energy ENDF/B-V cross sections was run using 1020 generations of neutrons with 1000 neutrons each. Twenty generations were skipped before averaging, so the result is the average of 1,000,000 neutron histories.

MCNP Input Listing for Case 1 of Table 13.b.

```
leu-sol-therm-005-01
   1  0              4:-5:10             imp:n=0
   2  3  8.701954E-02  -4 5 -10 (3:-6)      imp:n=1
   3  2  1.001130E-01  -3 6 -9 (2:-7)       imp:n=1
   4  0              -3 2 9 -10          imp:n=1
   5  3  8.701954E-02  -2 7 -10 (1:-8)      imp:n=1
   6  1  9.884795E-02  -1 11 8 -201         imp:n=1
   7  0              -1 11 201 -10        imp:n=1
   8  0              -11 8 -10           imp:n=1  fill=100
c
  100  0  -401 402 -403 404  imp:n=1  lat=1  u=100
        fill=-6:6 -6:6 0:0
                                      1 18r
                 1 2 2 2 2 1               1  5r
                2 2 2 2 2 2 2              1  4r
               2 2 2 2 2 2 2 2             1  3r
              2 2 2 2 2 2 2 2 2            1  2r
             2 2 2 2 2 2 2 2 2 2           1  1r
            1 2 2 2 2 2 2 2 2 2 1          1  1r
             2 2 2 2 2 2 2 2 2 2           1  2r
              2 2 2 2 2 2 2 2 2            1  3r
               2 2 2 2 2 2 2 2             1  4r
                2 2 2 2 2 2 2              1  5r
                 1 2 2 2 2 1               1 18r
c
 1000  3  8.701954E-02              -200  imp:n=1  u=1
 1001  1  9.884795E-02           200 -201  imp:n=1  u=1
 1002  0                       201       imp:n=1  u=1
c
 2000  1  9.884795E-02      -300     -200  imp:n=1  u=2
 2001  3  8.701954E-02   300         -200  imp:n=1  u=2
 2003  1  9.884795E-02           200 -201  imp:n=1  u=2
 2004  0                       201       imp:n=1  u=2
c
 3000  3  8.701954E-02      -302     -303  imp:n=1  u=3
 3001  4  6.811600E-02      -302  303      imp:n=1  u=3
 3002  3  8.701954E-02   302 -301          imp:n=1  u=3
 3003  1  9.884795E-02   301 -300     -200  imp:n=1  u=3
 3004  3  8.701954E-02   300          -200  imp:n=1  u=3
 3005  1  9.884795E-02   301       200 -201  imp:n=1  u=3
 3006  0               301       201       imp:n=1  u=3

   1  cz   55.
   2  cz   55.6
   3  cz   99.2
   4  cz  100.
c
   5  pz  -38.5
   6  pz  -37.5
   7  pz   -1.5
   8  pz    0.
   9  pz  108.       $ water level
  10  pz  248.5
c
  11  cz   54.8
c
  200  pz    1.7
  201  pz   58.9839    $ solution level
c
  300  cz    2.775
  301  cz    2.75
  302  cz    2.25
  303  pz    0.7
c
```

MCNP Input Listing for Case 1 of Table 13.b (cont'd).

```
 401  p   1.732050807569  -1  0   9.179869280115
 402  p   1.732050807569  -1  0  -9.179869280115
 403  py  4.589934640058
 404  py -4.589934640058

  m1  92234.50c  3.0893E-07
      92235.50c  5.7830E-05
      92236.50c  5.1050E-07
      92238.50c  9.5450E-04
       7014.50c  2.9898E-03
       8016.50c  3.8624E-02
       1001.50c  5.6221E-02
  m2   8016.50c  3.3371E-02
       1001.50c  6.6742E-02
  m3  26000.50c  5.9088E-02
      24000.50c  1.6532E-02
      28000.50c  8.1369E-03
      25055.50c  1.3039E-03
      14000.50c  1.3603E-03
      22000.50c  5.9844E-04
  m4   5010.50c  1.0844E-02
       5011.50c  4.3649E-02
       6012.50c  1.3623E-02
 mt1   lwtr.01t
 mt2   lwtr.01t
kcode  1000 1.0 20 1020
 sdef  pos=0. 0. 30. axs=0 0 1 rad=d1 ext=d2
  si1  0. 55.
  si2  30.
prdmp  3j 1
print
```

LEU-SOL-THERM-005

MCNP Input Listing for Case 2 of Table 13.b.

```
leu-sol-therm-005-02
   1  0              4:-5:10             imp:n=0
   2  3  8.701954E-02  -4 5 -10 (3:-6)      imp:n=1
   3  2  1.001130E-01  -3 6 -9 (2:-7)       imp:n=1
   4  0              -3 2 9 -10          imp:n=1
   5  3  8.701954E-02  -2 7 -10 (1:-8)      imp:n=1
   6  1  9.884795E-02  -1 11 8 -201         imp:n=1
   7  0              -1 11 201 -10        imp:n=1
   8  0              -11 8 -10           imp:n=1  fill=100
c
  100  0  -401 402 -403 404  imp:n=1  lat=1  u=100
        fill=-6:6 -6:6 0:0
                                      1 18r
                 1 2 2 2 2 1                1  5r
                2 2 2 2 2 2 2               1  4r
               2 2 2 2 2 2 2 2              1  3r
              2 2 2 2 2 2 2 2 2             1  2r
             2 2 2 2 2 2 2 2 2 2            1  1r
            1 2 2 2 2 3 2 2 2 2 1           1  1r
             2 2 2 2 2 2 2 2 2 2            1  2r
              2 2 2 2 2 2 2 2 2             1  3r
               2 2 2 2 2 2 2 2              1  4r
                2 2 2 2 2 2 2               1  5r
                 1 2 2 2 2 1                1 18r
c
 1000  3  8.701954E-02              -200  imp:n=1  u=1
 1001  1  9.884795E-02           200 -201  imp:n=1  u=1
 1002  0                       201       imp:n=1  u=1
c
 2000  1  9.884795E-02      -300     -200  imp:n=1  u=2
 2001  3  8.701954E-02   300         -200  imp:n=1  u=2
 2003  1  9.884795E-02           200 -201  imp:n=1  u=2
 2004  0                       201       imp:n=1  u=2
c
 3000  3  8.701954E-02      -302     -303  imp:n=1  u=3
 3001  4  6.811600E-02      -302  303       imp:n=1  u=3
 3002  3  8.701954E-02   302 -301           imp:n=1  u=3
 3003  1  9.884795E-02   301 -300     -200  imp:n=1  u=3
 3004  3  8.701954E-02   300          -200  imp:n=1  u=3
 3005  1  9.884795E-02   301       200 -201  imp:n=1  u=3
 3006  0               301       201       imp:n=1  u=3

   1  cz   55.
   2  cz   55.6
   3  cz   99.2
   4  cz  100.
c
   5  pz  -38.5
   6  pz  -37.5
   7  pz   -1.5
   8  pz    0.
   9  pz  108.       $ water level
  10  pz  248.5
c
  11  cz   54.8
c
  200  pz    1.7
  201  pz   65.2501    $ solution level
c
  300  cz    2.775
  301  cz    2.75
  302  cz    2.25
  303  pz    0.7
```

MCNP Input Listing for Case 2 of Table 13.b (cont'd).

```
c
  401  p   1.732050807569  -1  0   9.179869280115
  402  p   1.732050807569  -1  0  -9.179869280115
  403  py  4.589934640058
  404  py -4.589934640058

   m1  92234.50c  3.0893E-07
       92235.50c  5.7830E-05
       92236.50c  5.1050E-07
       92238.50c  9.5450E-04
        7014.50c  2.9898E-03
        8016.50c  3.8624E-02
        1001.50c  5.6221E-02
   m2   8016.50c  3.3371E-02
        1001.50c  6.6742E-02
   m3  26000.50c  5.9088E-02
       24000.50c  1.6532E-02
       28000.50c  8.1369E-03
       25055.50c  1.3039E-03
       14000.50c  1.3603E-03
       22000.50c  5.9844E-04
   m4   5010.50c  1.0844E-02
        5011.50c  4.3649E-02
        6012.50c  1.3623E-02
  mt1   lwtr.01t
  mt2   lwtr.01t
kcode  1000 1.0 20 1020
 sdef  pos=0. 0. 33. axs=0 0 1 rad=d1 ext=d2
  si1  0. 55.
  si2  33.
prdmp  3j 1
print
```

MCNP Input Listing for Case 3 of Table 13.b.

```
leu-sol-therm-005-03
   1  0              4:-5:10             imp:n=0
   2  3  8.701954E-02  -4 5 -10 (3:-6)      imp:n=1
   3  2  1.001130E-01  -3 6 -9 (2:-7)       imp:n=1
   4  0              -3 2 9 -10          imp:n=1
   5  3  8.701954E-02  -2 7 -10 (1:-8)      imp:n=1
   6  1  9.884795E-02  -1 11 8 -201         imp:n=1
   7  0              -1 11 201 -10        imp:n=1
   8  0              -11 8 -10           imp:n=1  fill=100
c
  100  0  -401 402 -403 404  imp:n=1  lat=1  u=100
        fill=-6:6 -6:6 0:0
                                      1 18r
                 1 2 2 2 2 1                1  5r
                2 2 2 2 2 2 2               1  4r
               2 2 3 2 2 3 2 2              1  3r
              2 2 2 2 2 2 2 2 2             1  2r
             2 2 2 2 2 2 2 2 2 2            1  1r
            1 2 3 2 2 3 2 2 3 2 1           1  1r
             2 2 2 2 2 2 2 2 2 2            1  2r
              2 2 2 2 2 2 2 2 2             1  3r
               2 2 3 2 2 3 2 2              1  4r
                2 2 2 2 2 2 2               1  5r
                 1 2 2 2 2 1                1 18r
c
 1000  3  8.701954E-02              -200  imp:n=1  u=1
 1001  1  9.884795E-02           200 -201  imp:n=1  u=1
 1002  0                       201       imp:n=1  u=1
c
 2000  1  9.884795E-02      -300     -200  imp:n=1  u=2
 2001  3  8.701954E-02   300         -200  imp:n=1  u=2
 2003  1  9.884795E-02           200 -201  imp:n=1  u=2
 2004  0                       201       imp:n=1  u=2
c
 3000  3  8.701954E-02      -302     -303  imp:n=1  u=3
 3001  4  6.811600E-02      -302  303      imp:n=1  u=3
 3002  3  8.701954E-02   302 -301          imp:n=1  u=3
 3003  1  9.884795E-02   301 -300     -200  imp:n=1  u=3
 3004  3  8.701954E-02   300          -200  imp:n=1  u=3
 3005  1  9.884795E-02   301       200 -201  imp:n=1  u=3
 3006  0               301       201       imp:n=1  u=3

   1  cz   55.
   2  cz   55.6
   3  cz   99.2
   4  cz  100.
c
   5  pz  -38.5
   6  pz  -37.5
   7  pz   -1.5
   8  pz    0.
   9  pz  108.       $ water level
  10  pz  248.5
c
  11  cz   54.8
c
  200  pz    1.7
  201  pz  106.6233    $ solution level
c
  300  cz    2.775
  301  cz    2.75
  302  cz    2.25
  303  pz    0.7
c
```

MCNP Input Listing for Case 3 of Table 13.b (cont'd).

```
 401  p   1.732050807569  -1  0   9.179869280115
 402  p   1.732050807569  -1  0  -9.179869280115
 403  py  4.589934640058
 404  py -4.589934640058

  m1  92234.50c  3.0893E-07
      92235.50c  5.7830E-05
      92236.50c  5.1050E-07
      92238.50c  9.5450E-04
       7014.50c  2.9898E-03
       8016.50c  3.8624E-02
       1001.50c  5.6221E-02
  m2   8016.50c  3.3371E-02
       1001.50c  6.6742E-02
  m3  26000.50c  5.9088E-02
      24000.50c  1.6532E-02
      28000.50c  8.1369E-03
      25055.50c  1.3039E-03
      14000.50c  1.3603E-03
      22000.50c  5.9844E-04
  m4   5010.50c  1.0844E-02
       5011.50c  4.3649E-02
       6012.50c  1.3623E-02
 mt1   lwtr.01t
 mt2   lwtr.01t
kcode  1000 1.0 20 1020
 sdef  pos=0. 0. 54. axs=0 0 1 rad=d1 ext=d2
  si1  0. 55.
  si2  54.
prdmp  3j 1
print
```